Hybrid Cascaded H-Bridge Multilevel Inverter Motor Drive DTC Control for Electric Vehicles

Farid Khoucha, Soumia Mouna Lagoun, Khoudir Marouani, Abdelaziz Kheloui, Mohamed Benbouzid

Hybrid Cascaded H-Bridge Multilevel Inverter Motor Drive DTC Control for Electric Vehicles

F. Khoucha[1,2], S.M. Lagoun[2], K. Marouani[2], A. Kheloui[2] and M.E.H. Benbouzid[1]
[1]Laboratoire Brestois de Mécanique et des Systèmes (LBMS – EA 4325), University of Brest
IUT of Brest – Rue de Kergoat – CS 93837, 29238 Brest Cedex 03, France
E-mail: m.benbouzid@ieee.org
[2]Electrical Engineering Department, Polytechnic Military Academy, 16111 Algiers, Algeria.

***Abstract*—This paper presents a hybrid cascaded H-bridge multilevel motor drive DTC control scheme for Electric (EV) or Hybrid Electric Vehicles (HEV). The control method is based on Direct Torque Control operating principles. The stator voltage vector reference is computed from the stator flux and torque errors imposed by the flux and torque controllers. This voltage reference is then generated using a hybrid cascaded H-bridge multilevel inverter, where each phase of the inverter can be implemented using a DC source, which would be available from fuel cells, batteries, or ultracapacitors. This inverter provides nearly sinusoidal voltages with very low distortion, using less switching devices. Due to the small *dv/dt*'s, torque ripple is greatly reduced. In addition, the multilevel inverter can generate a high and fixed switching frequency output voltage with less switching losses, since only the small power cells of the inverter operate at high switching rate. Therefore a high performance and also efficient torque and flux controller is obtained, enabling a DTC solution for multilevel inverter powered motor drives.**

***Index Terms*—AC drives, Direct Torque Control (DTC), multilevel inverters.**

I. Introduction

Multilevel voltage-source inverters are intensively studied for high-power applications [1-2], and standard drives for medium-voltage industrial applications have become available [3-4]. Solutions with a higher number of output voltage levels have the ability to synthesize waveforms with a better harmonic spectrum and to limit the motor-winding insulation stress. However, their increasing number of devices tends to reduce the overall reliability and efficiency of the power converter. On the other hand, solutions with a low number of levels either need a rather large and expensive LC output filter to limit the motor-winding insulation stress or can only be used with motors that do withstand such stress.

Most investigations concerned topologies with the same voltage rating for all devices. Advantages of such symmetric multilevel converters are modularity and control simplicity. Hybrid multilevel inverters use different intermediate circuit capacitor voltages in various parts of the inverter. By addition and subtraction of these voltages, more different output voltage levels can be generated with the same number of components, compared to a symmetric multilevel inverter [5-8]. Higher output quality can be obtained with smaller circuit and control complexity, and output filters can be remarkably shrunk or even eliminated.

One of the methods that have been used by one major manufacturer in multilevel-level inverters is DTC, which is recognized today as a high-performance control strategy for AC drives [9-15]. Several authors have addressed the problem of improving the behavior of DTC AC motors, especially by reducing the torque ripple. Different approaches have been proposed [9]: improving the look-up table; varying the hysteresis bandwidth of the torque controller, using flux, torque and speed observers. Although these approaches are well suitable for the classical two levels inverter, their extension to a greater number of levels is not easy. Throughout this paper, a theoretical background is used to design a strategy compatible with hybrid cascaded H-bridge multilevel inverter. It allows not only controlling the electromagnetic state of the motor with improved performance (minimization of the torque ripple), but also to control the switching frequency and flying capacitors voltages.

II. Cascaded H-Bridges Structure and Operation

The hybrid cascaded H-bridge inverter power circuit is illustrated in Fig. 1. The inverter is composed of three legs, in each one a series connection of two H-bridge inverters fed by independent DC sources that are not equal ($V_1 < V_2$). Indeed, it may be obtained from batteries, fuel cells, or ultracapacitors in EVs or HEVs [16-18].

The use of asymmetric input voltages can reduce, or when properly chosen, eliminate redundant output levels, maximizing the number of different levels generated by the inverter. Therefore this topology can achieve the same output voltage quality with less number of semiconductors. This also reduces volume, costs, and losses and improves reliability. When cascading two level inverters like H-bridges, the optimal asymmetry is obtained by using voltage sources proportionally scaled to the two H-bridges power.

Particular cell i can generate three levels ($+V_i$, 0, $-V_i$). The total inverter output voltage for a particular phase j is defined by

$$v_{jN} = \sum_{i=1}^{m} v_{ji} = \sum_{i=1}^{m} V_i \left(S_{i1} - S_{i2}\right),\ j \in \{a,\ b,\ c\} \tag{1}$$

Where v_{ij} is the i cell output voltage, m is the number of cells per phase, and (S_{i1}, S_{i2}) the switching state associated to the i cell. Equation (1) explicitly shows how the output voltage of one cell is defined by one of the four binary combinations of switching state, with "1" and "0" representing the "ON" and "OFF" state of the corresponding switch, respectively.

978-1-4244-1736-0/08/$25.00 ©2008 IEEE

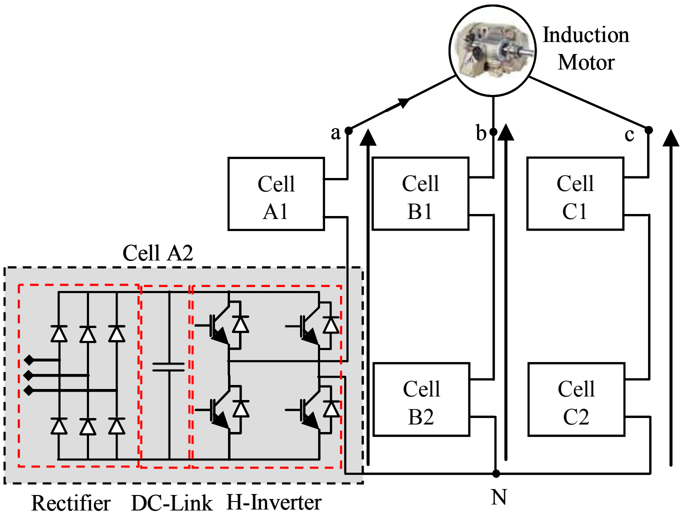

Fig. 1. Asymmetric cascaded H-bridge multilevel inverter.

The optimal asymmetry is obtained with DC links scaled in powers of two or three, generating 7 (Fig. 2) or 9 (Fig. 3) different output levels. 9 different output levels can be generated using only two cells (8 switches) while four cells (16 switches) are necessary to achieve the same amount of level with symmetric fed inverter.

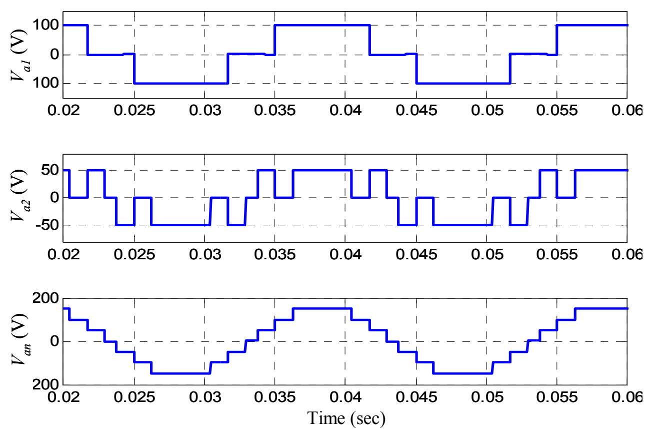

Fig. 2. Asymmetric multilevel inverter with 7-levels output voltage synthesis.

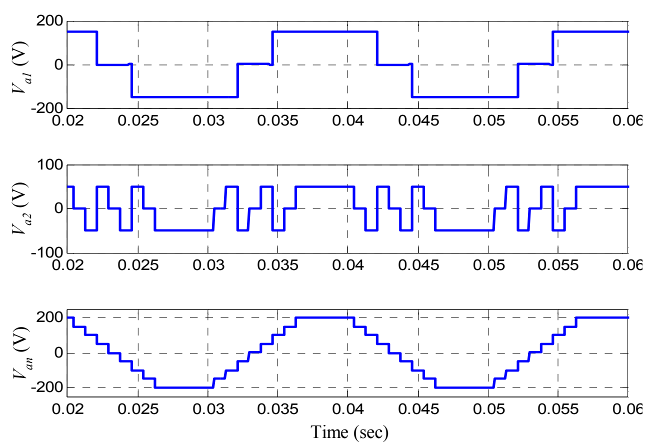

Fig. 3. Asymmetric multilevel inverter with 9-levels output voltage synthesis.

III. Induction Motor DTC

DTC is an alternative method to flux oriented control [10]. The basic principle is the direct selection of a space vector and corresponding control signals, in order to instantaneously regulate the electromagnetic torque and stator flux magnitudes. Several advantages may be considered: higher robustness regarding motor parameter variations, higher torque dynamics, easier flux and speed estimators implementation since no rotational transformations are required. However, in the standard version, important torque ripple is obtained even at high sampling frequencies. Moreover, the converter switching frequency is inherently variable and very dependent on torque and shaft speed. This produces torque harmonics with variable frequencies and an acoustic noise with disturbance intensities very dependent on these mechanical variables and particularly grating at low speed. The additional degrees of freedom (space vectors, phase configurations, etc.) provided by the multilevel inverter should therefore be exploited by the control strategy in order to reduce these drawbacks.

A. Nomenclature

v_s = Stator voltage vector;
ϕ_s (ϕ_r) = Stator (rotor) flux vector;
T_e = Electromagnetic torque;
R_s = Stator resistance;
L_s (L_r) = Stator (rotor) inductance;
L_m = Magnetizing inductance;
σ = Total leakage coefficient, $\sigma = 1 - L_m^2/L_sL_r$;
θ_{sr} = Angle between stator and rotor flux vectors;
p = pole pair number.

A. Torque and Flux Estimation

The stator flux vector an induction motor is related to the stator voltage and current vectors by

$$\frac{d\phi_s(t)}{dt} = v_s(t) - R_s i_s(t) \qquad (2)$$

Maintaining v_s constant over a sample time interval and neglecting the stator resistance, the integration of (2) yields

$$\Delta\phi_s(t) = \phi_s(t) - \phi_s(t-\Delta t) = \int_{t-\Delta t}^{t} v_s \Delta t \qquad (3)$$

Equation (3) reveals that the stator flux vector is directly affected by variations on the stator voltage vector. On the contrary, the influence of v_s over the rotor flux is filtered by the rotor and stator leakage inductance [19], and is, therefore, not relevant over a short-time horizon. Since the stator flux can be changed quickly while the rotor flux rotates slower, the angle between both vectors θ_{sr} can be controlled directly by v_s. A graphical representation of the stator and rotor flux dynamic behavior is illustrated in Fig. 4. The exact relationship between stator and rotor flux shows that keeping the amplitude of ϕ_s constant will produce a constant flux ϕ_r [20].

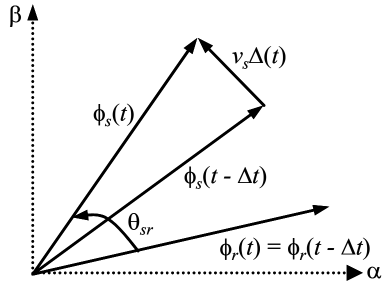

Fig. 4. Influence of v_s over ϕ_s during a simple interval Δt.

Since the electromagnetic torque developed by an induction motor can be expressed by [20]

$$T_e = \frac{3}{2} p \frac{L_m}{\sigma L_s L_r} \phi_s \phi_r \sin \theta_{sr} \tag{4}$$

It follows that change in θ_{sr} due to the action of v_s allows for direct and fast change in the developed torque.

DTC uses this principle to achieve the induction motor desired torque response, by applying the appropriate stator voltage vector to correct the flux trajectory.

B. Voltage Vector Selection

Figure 5 illustrates one of the 127 voltage vectors generated by the inverter at instant $t = k$, denoted by v_s^k (central dot). The next voltage vector to be applied to the load v_s^{k+1}, can be expressed by

$$v_s^{k+1} = v_s^k + \Delta v_s^k \tag{5}$$

where $\Delta v_s^k = \{v_i \mid i = 1, \ldots, 6\}$. Each vector v_i corresponds to one corner of the elemental hexagon illustrated in gray and by the dashed line in Fig. 5. The task is to determine which v_s^{k+1} will correct the torque and flux responses, knowing the actual voltage vector v_s^k, the torque and flux errors e_ϕ^k and e_T^k and the stator flux vector position (sector determined by angle θ_s). Note that the next voltage vector v_s^{k+1} applied to the load will always be one of the six closest vectors to the previous v_s^k, this will soften the actuation effort and reduce high dynamics in torque response due to possible large changes in the reference.

Using (4) and (5), and analyzing, for example, sector (2) illustrated in Fig. 6; the application of v_1 increases the stator flux amplitude but reduces θ_{sr} leading to a torque reduction. Conversely, v_4 reduces the flux magnitude, while it increases θ_{sr} and thus the torque. If v_3 is applied to the load, both torque and flux increase, and it is clear that v_6 produces the inverse effect. Table 1 summarizes vector selections according to the above criterion, for the different sectors and comparators output (desired ϕ_s and T_e corrections).

To implement the DTC of the induction motor fed by an hybrid H-bridge multilevel inverter, one should determine at each sampling period the logic state of the inverter switches as a function of instantaneous values of torque and flux for the selection of the space vector, in the α-β frame.

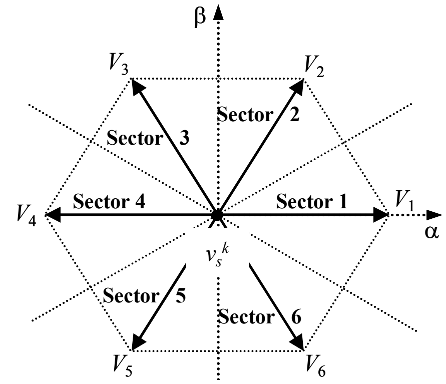

Fig. 5. Possible voltage changes Δv_s^k that can be applied from certain v_s^k.

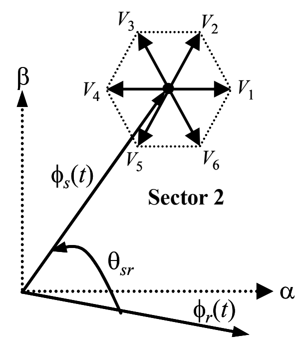

Fig. 6. Voltage selection Δv_s^k in sector 2.

Table 1. Voltage vector selection lookup table.

Sector	sign(e_ϕ^k,e_T^k)			
	(+,+)	(+,–)	(–,+)	(–,–)
1	V_2	V_6	V_3	V_5
2	V_3	V_1	V_4	V_6
3	V_4	V_2	V_5	V_1
4	V_5	V_3	V_6	V_2
5	V_6	V_4	V_1	V_3
6	V_1	V_5	V_2	V_4

Once the space is chosen, the sequence of phase levels can be selected. To ensure this task, one should detect the position of the space vector in α-β frame (Q^k at sampling time t^k). The proposed algorithm must then select the next position Q^{k+1} to be achieved before next sampling instant t^{k+1} (Fig. 7) in order to reduce voltage steps magnitude. This task allows the commutation number reduction in the same phase order to minimize losses and consequently the torque ripple. Finally, the configuration of each phase will be selected and must be able to generate the phase levels.

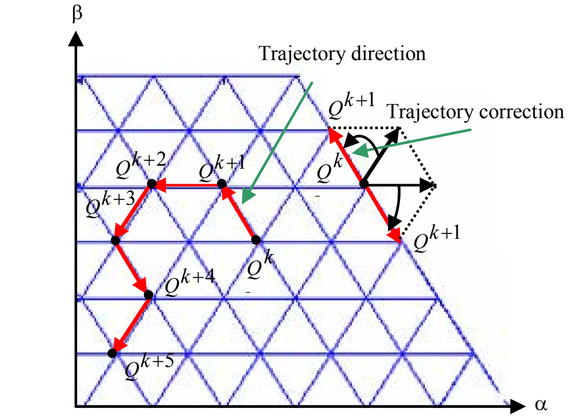

Fig. 7. Optimal space vector tracking and trajectory correction in the stationary αβ frame.

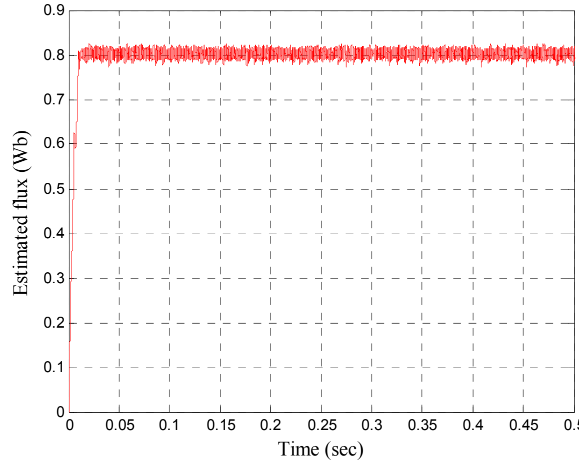

(b) Stator flux waveform.

IV. Simulation and Experimental Results

For the validation of the above discussed control approach, simulations and experiments have been carried out. Figure 8 shows simulation results for a 7-level cascaded H-bridge inverter. For further verification, a three-phase DSP (TMS320LF2407A) controlled 7-level cascaded H-bridge multilevel DTC induction motor drive system prototype was built and tested (Fig. 9). The induction motor was rated at 1-kW / 380V / 5.2 A / 1420 rpm. The control cycle is 120 µs. It should be noted, as illustrated by Fig. 9a, that the experimental setup was built to slightly emulate an EV.

Figure 10 illustrates experimental results of the 7-level inverter realized in the laboratory (Fig. 9). The output voltages form with 7-level stepped multilevel waveform can be clearly appreciated; the motor currents complete the overview of the performance of the drive. They appear completely sinusoidal, since the low pass nature of the load has filtered the high frequency content of the applied voltage. The stator flux with constant amplitude imposed by the flux controller confirms the good dynamic performance of the drive. The most important results is that torque ripple has been almost eliminated in comparison to two level classic DTC [21].

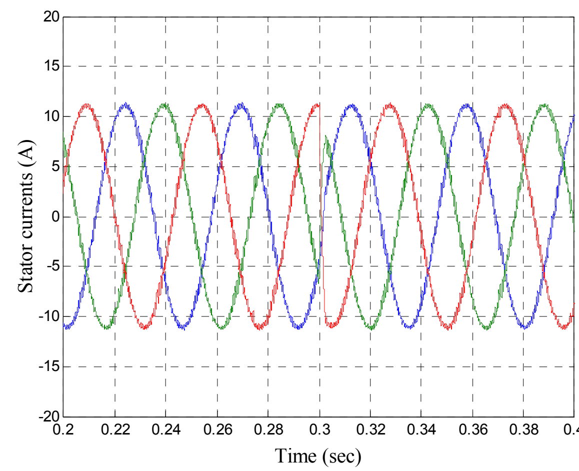

(c) Output current waveform.

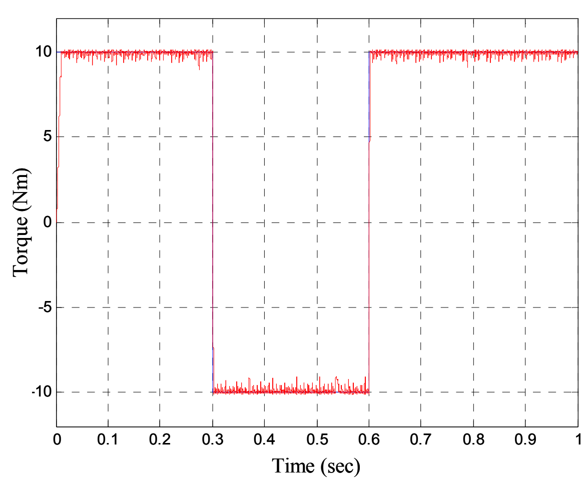

(a) Estimated torque waveform.

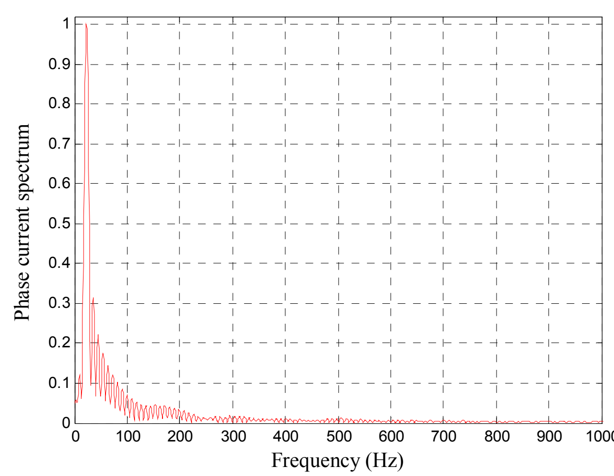

(d) Phase current FFT analysis.

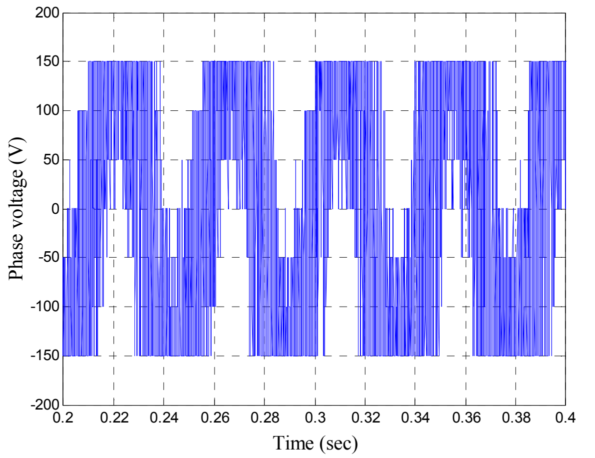

(e) Phase voltage waveform (7 levels).

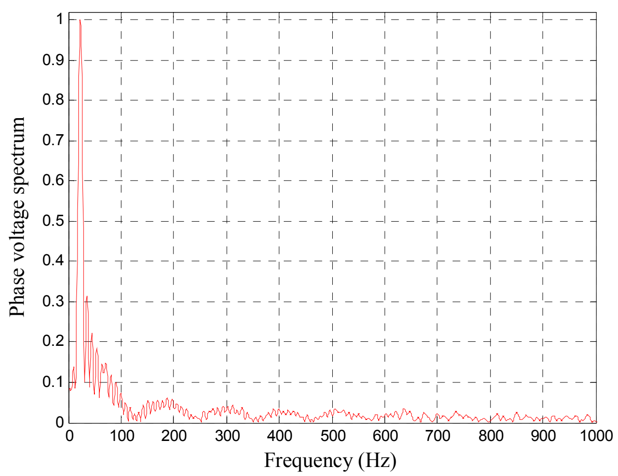

(f) Phase voltage FFT analysis.

Fig. 8. 7-level cascaded H-bridge inverter simulation results.

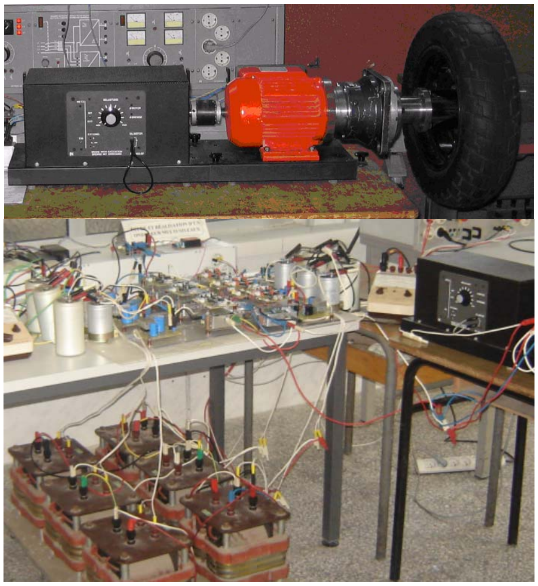

(a)

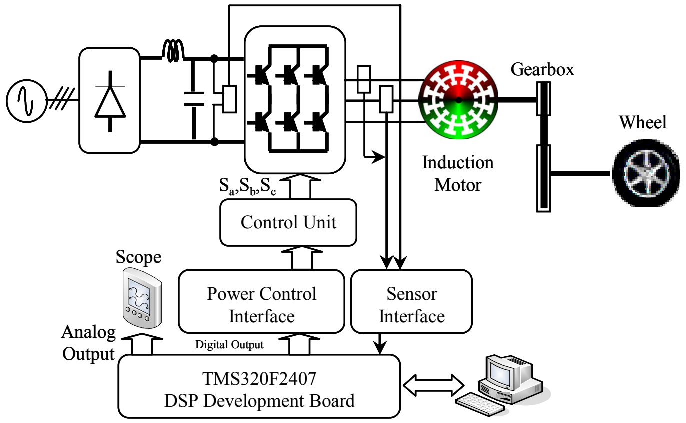

(b)

Fig. 9. The experimental setup.

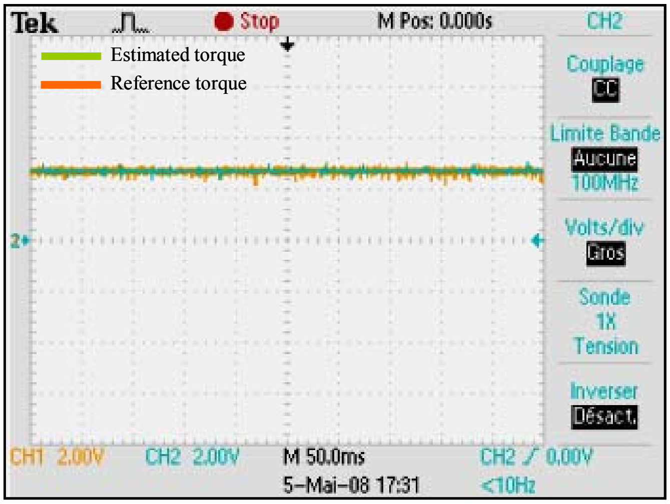

(a) Reference and estimated torque waveforms.

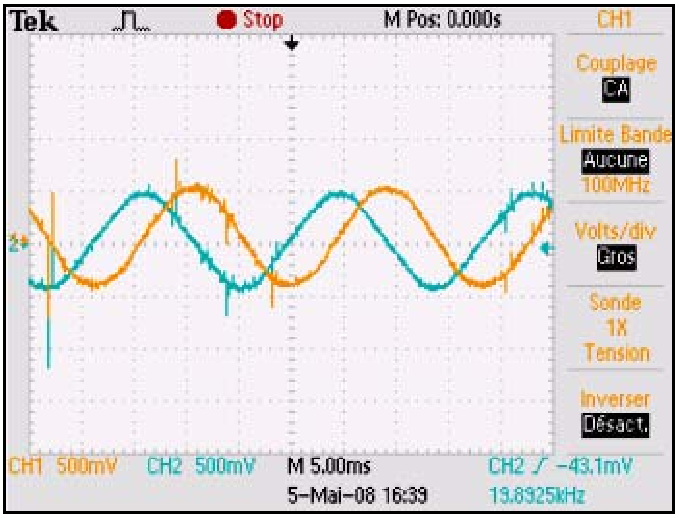

(b) α-β flux component waveforms.

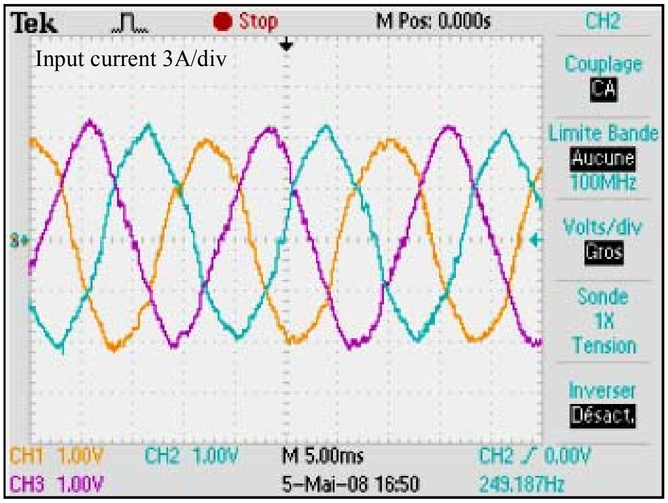

(c) Output current waveforms.

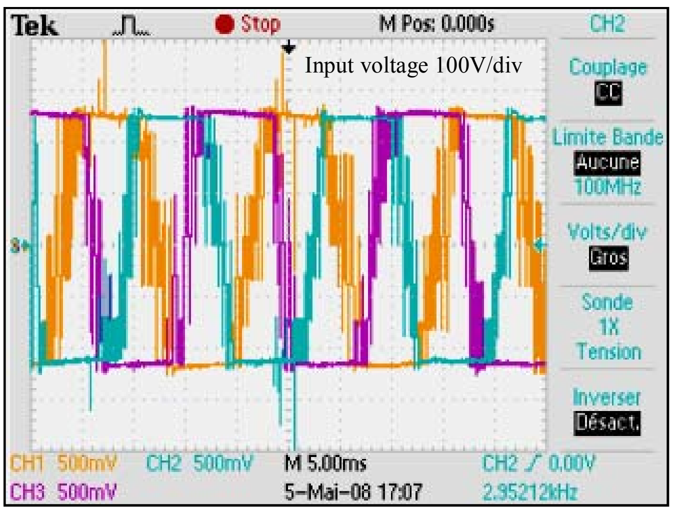

(d) Multilevel inverter output voltages during DTC.

Fig. 10. 7-level cascaded H-bridge inverter experimental results.

V. Conclusion

This paper dealt with a hybrid cascaded H-bridge multilevel motor drive DTC control scheme that has big potential for Electric (EVs) or Hybrid Electric Vehicles (HEVs). The main achievements of the proposed control method are: significant reduction in the torque ripple, sinusoidal output voltages and currents, lower switching losses and a high-performance torque and flux regulation. The hybrid multilevel inverter enables a DTC solution for high-power motor drives, not only due to the higher voltage capability provided by multilevel inverters, but mainly due to the reduced switching losses and the improved output voltage quality, which provides sinusoidal current without output filter.

References

[1] L.G. Franquelo et *al.*, “The age of multilevel converters arrives, *IEEE Industrial Electronics Magazine*,” vol. 2, n°2, pp. 28-39, June 2008.

[2] J. Rodriguez et *al.*, “Multilevel inverters: A survey of topologies, controls and applications,” *IEEE Trans. Industrial Electronics,* vol. 49, n°4, pp. 724-738, August 2002.

[3] M. Escalante et *al.*, “Flying capacitor multilevel inverters and DTC motor drive applications,” *IEEE Trans. Industrial Electronics*, vol. 49, n°4, pp. 805-815, August 2002.

[4] T. Ishida et *al.*, “Fundamental characteristics of five-level double converters with adjustable DC voltages for induction motor drives,” *IEEE Trans. Industrial Electronics*, vol. 49, n°4, pp. 775-782, August 2002.

[5] C. Rech et *al.*, “Hybrid multilevel converters: Unified analysis and design considerations, *IEEE Trans. Industrial Electronics*,” vol. 54, n°2, pp. 1092-1104, April 2007.

[6] M. Veenstra et *al.*, “Control of a hybrid asymmetric multilevel inverter for competitive medium-voltage industrial drives, *IEEE Trans. Industry Applications*,” vol. 41, n°2, pp. 655-664, March-April 2005.

[7] P.C. Loh et *al.*, “Modular hysteresis current control of hybrid multilevel inverters,” *IEE Proc. Electric Power Applications*, vol. 152, n°1, pp. 1-8, January 2005.

[8] Y.S. Lai et *al.*, “Topology for hybrid multilevel inverter, *IEE Proc. Electric Power Applications*,” vol. 149, n°6, pp. 449-458, November 2002.

[9] G.S. Buga et *al.*, “Direct torque control of PWM inverter-fed AC motors - A survey, *IEEE Trans. Industrial Electronics*,” vol. 51, n°4, pp. 744-757, August 2004.

[10] D. Casadei et *al.*, “FOC and DTC: two viable schemes for induction motors torque control,” *IEEE Trans. Power Electronics*, vol. 17, n°5, pp. 779-787, September 2002.

[11] M.E.H. Benbouzid et *al.*, “A loss-minimization DTC scheme for EV induction motors,” *IEEE Trans. Vehicular Technology*, vol. 56, n°1, pp. 81-88, January 2007.

[12] J. Faiz et *al.*, “Sensorless direct torque control of induction motors used in electric vehicle,” *IEEE Trans. Energy Conversion*, vol. 18, n°1, pp. 1-10, March 2003.

[13] X. del Toro Garcia et *al.*, “Direct torque control of induction motors utilizing three-level voltage source inverters,” *IEEE Trans. Industrial Electronics*, vol. 55, n°2, pp. 965-958, February 2008.

[14] J. Rodriguez et *al.*, “Direct torque control with imposed switching frequency in an 11-level cascaded inverter,” *IEEE Trans. Industrial Electronics*, vol. 51, n°4, pp. 827-833, August 2008.

[15] S. Kouro et *al.*, “High-performance torque and flux control for multilevel inverter fed induction motors,” *IEEE Trans. Power Electronics*, vol. 22, n°6, pp. 2116-2123, November 2007.

[16] M. Carpita et *al.*, “Multilevel converter for traction applications: Small-scale prototype tests results,” *IEEE Trans. Industrial Electronics*, vol. 55, n°5, pp. 2203-2212, May 2008.

[17] S. Lu et *al.*, “A unique ultracapacitor direct integration scheme in multilevel motor drives for large vehicle propulsion,” *IEEE Trans. Vehicular Technology*, vol. 56, n°4, Part 1, pp. 1506-1515, July 2007.

[18] S. Dieckerhoff et *al.*, “Power loss-oriented evaluation of high voltage IGBTs and multilevel converters in transformerless traction applications, *IEEE Trans. Power Electronics*,” vol. 20, n°6, pp. 1328-1336, November 2005.

[19] D. Casadei et *al.*, “DTC drives for wide speed range applications using a robust flux-weakening algorithm,” *IEEE Trans. Industrial Electronics*,” vol. 54, n°5, pp. 2451-24-61, October 2007.

[20] M. Escalante et *al.*, “Flying capacitor multilevel inverters and DTC motor drive applications,” *IEEE Trans. Industrial Electronics*, vol. 49, n°4, pp. 805-815, August 2002.

[21] F. Khoucha et *al.*, “An improved sensorless DTC scheme for EV induction motors,” *in Proceedings of the IEEE IEMDC'07*, Antalya (Turkey), vol. 2, pp. 1159-1164, May 2007.

[22] F. Khoucha et *al.*, “A minimization of speed ripple of sensorless DTC for controlled induction motors used in electric vehicles,” *in Proceedings of the IEEE IECON'06*, Paris (France), pp. 1339-1344, November 2006.